Publisher: GSA
Journal: GEOL: Geology
DOI:10.1130/G45277.1

Entrained sand generates fault plane reflections on a deep-water thrust zone

Yukitsugu Totake[1,2*], Robert W. H. Butler[1], Clare E. Bond[1], Hiroyuki Tokunaga[2], and Aznan Aziz[3]

[1]*Geology and Petroleum Geology, School of Geosciences, University of Aberdeen, Kings College, Aberdeen AB24 3FX, UK*

[2]*Subsurface Evaluation Unit, Technical Division, INPEX CORPORATION, Tokyo 107-6332, Japan*

[3]*Resource Exploration Department, PETRONAS, 50088 Kuala Lumpur, Malaysia*

*E-mails: yukitsugu.totake@inpex.co.jp

ABSTRACT

Thrust zones in a deep-water fold-thrust belt, offshore NW Borneo, display prominent reflections that can be mapped through a 3D seismic volume. Unlike fault-plane reflections obtained from thrusts in other systems, these have positive polarity. Well data show that the reflections in the Borneo data set originate from fault-bound sandstone slices, with porosity-occluding calcite cement, entrained along the thrust zone. The thrust zone can support elevated fluid pressures beneath the fault with the cemented sandstones. Multiple sandstone slices indicate complex patterns of thrust zone localization, perhaps a common feature for deformation in sedimentary multilayers typical of many deep-water depositional successions.

INTRODUCTION

Thrust faults are not generally imaged on seismic reflection data but are interpreted from terminations and offsets of stratal reflectors. Rare examples of direct reflections from fault zones through sedimentary rocks are reported and conventionally attributed to over-pressured pore fluids along the fault zones (e.g., Park et al., 2002). However, many published interpretations are limited by the lack of well-penetrations so that the petrophysical response remains conjectural. Structural complexities of individual thrusts are commonly ignored in seismic data – with zones of finite deformation simplified as single discrete surfaces. These simplifications may prevent a better understanding of the geometry of thrust zones and their physical properties in the subsurface (Iacopini et al., 2016). Here we relate seismic imaging to petrophysical character, determined through a well-penetration, of a thrust zone in a turbidite sequence to infer processes of thrust zone development and resulting fault zone architectures.

Detailed descriptions of the structural and lithological complexity of brittle fault zones come from field studies and laboratory experiments, chiefly of normal faults (reviewed by Faulkner et al., 2010). The complexity of fault zones arises from combinations of factors such as host rock lithology, fault displacement, segment linkage, strain localization, and fluid-rock interaction (Childs et al., 2009; Shipton and Cowie, 2001; Caine et al., 1996). Consequently, natural fault zones exhibit diverse attributes and dimensions (e.g., Torabi and Berg, 2011), with abrupt property variations in space (e.g., Shipton and Cowie, 2003). A 3D characterization of individual fault zones using direct observational data alone is highly challenging and uncertain (e.g., Torabi et al., 2016).

Since the 1990s, some complex sub-surface fault systems have been revealed using seismic attributes (see Chopra and Marfurt, 2005 for a historical review). These

Publisher: GSA
Journal: GEOL: Geology
DOI:10.1130/G45277.1

seismic attributes can be inferred to show spatial distributions of deformation interpreted as multiple fault strands (e.g., Iacopini et al., 2016). Characterization of internal fault zone properties using seismic data sets has also recently received attention (e.g., Kolyukhin et al., 2017). However, these subsurface interpretations and seismic characterizations have remained hypothetical without confirmation by direct sampling of thrust zones through drilling.

We combine subsurface data acquired from a hydrocarbon exploration well with seismic reflection data from the offshore NW Borneo. The seismic data reveals a prominent fault-plane reflection that can be mapped in this volume. The well that penetrated a thrust zone allows prediction of the petrophysical character of the thrust zone. We evaluate the hydraulic property of the thrust zone based on pore-pressure predictions from the well. Our subsurface interpretation is calibrated against outcrop examples to compare geometries and the development processes of thrust zones in turbidite successions.

SEISMIC DATA AND THE PRE-DRILLED INTERPRETATION

Offshore NW Borneo, Malaysia, contains a thrust system developed in a thick stack of turbidite sandstones and related claystones chiefly of Early Miocene to recent age (e.g., Hutchison, 2005; Fig. 1a). We use part of an 830 km2 3D seismic reflection survey that images three sub-parallel trains of fold-thrust structures along with industrial drilling data for structural mapping and lithology interpretation (Totake et al., 2018; Fig. 1a). For confidentiality reasons, specific names of both seismic and well data are not revealed here. The seismic data were acquired between September and December 2012 using 10 × 6 km PGS GeoStreamer® and a dual 4,130 in3 source. Data recording was repeated along three sail-line orientations, displaced by 60°. Processing of these multi-azimuth data sets using Kirchhoff pre-stack depth migration was completed in December 2013. The processed seismic volume has in-lines and cross-lines spaced at 12.5 m with the data record length of 7 s from mean sea level at a sampling rate of 2 ms.

The data volume shows excellent illuminations of multi-layered turbiditic sequences deformed into fold-thrust structures with pre-, syn-, and post-kinematic strata (Fig. 1b). The pre-kinematic strata, the lower section of the data volume (below h4 in Fig. 1b), show near constant thickness with large offsets of stratal reflections along thrust faults. Post-kinematic strata drape the deformed sequences with a constant thickness in the upper one second of the seismic data (above h7 in Fig. 1b). The syn-kinematic strata lie between these two sequences with abrupt variation in thickness. Here we consider one thrust zone that offsets the pre-kinematic strata. Part of the mapped thrust is decorated with a continuous positive-impedance reflection (white arrows in Fig. 1b). We termed this event X-reflector and mapped it through the data volume (Fig. 2). The X-reflector extends c. 1–2 km down the dip of the thrust zone. It is largely bounded top and bottom against a prominently reflective stratal package termed Fan A, identified on either side of the thrust zone (Fig. 2). The X-reflector continues for c. 16 km along strike, has a variable form with local segmentation. The origin of the X-reflector was unknown before drilling. However, its positive impedance character is not consistent with an origin in a layer of especially over-pressured strata, which generate negative polarities (e.g., Moore et al., 1995).

WELL DATA AND INTERPRETATION

A hydrocarbon exploration well named Well Z was drilled to test potential sub-thrust reservoirs from 31 December 2014 through 15 April 2015 (Fig. 3). Descriptions of cuttings were integrated with drilling parameters, and a spectrum of well log data (gamma ray, neutron/density, sonic, and resistivity) acquired using Logging While Drilling or LWD tools for determining lithology. XRD analysis of the cuttings and sidewall cores were used to control the lithological determinations. Electric wireline logs were also acquired to supplement the LWD log data and to record acoustic borehole images from which dipmeter data were collected. A synthetic seismogram was calculated following the standard methods (Schlumberger, 1991), using LWD sonic and density logs corrected with wireline logs.

From the sea-bed, the well penetrated Quaternary down to Upper Miocene sandstone-claystone alternations. A prominent stack of sandstones with a thickness of c. 290 m corresponds to a seismically reflective unit Fan A (Fig. 3). This was encountered twice in the well, confirming the stratigraphic repetition expected in the thrust interpretation based on the seismic data. These Upper Miocene sandstones vary in thickness from tens to a few meters and form 50-80 m thick packages. The claystones are typically tens of meters thick.

Approaching the X-reflector, the well-log responses change from the background trends with high-frequency responses in sonic together with a low gamma-ray signal (Fig. 3). Below the X-reflector the log responses return to the background trend. The thickness of the anomalous log-responses is 107 m in the well. This interval comprises 40 m of claystone underlain by two massive sandstones with thicknesses of 28 m and 26 m. The whole interval contains relatively abundant calcite veins found in the drill cuttings. Fe-calcite content determined by X-ray diffraction in the cuttings is generally high within the thrust zone (up to 11.7 weight%) (Fig. 3). Apart from these cements, both claystone and sandstones show characteristics of the turbiditic sequences found in intervals elsewhere in the Upper Miocene sequences in the well. The two massive sandstones show high resistivity and fast acoustic sonic logs (Fig. 3). These log responses are consistent with porosity in the sandstones being occluded by calcite cement. Good match between the synthetic seismogram and the 3D seismic data shows that the X-reflector derives from the top of these cemented sandstones (Fig. 3). We infer these bodies that are imaged in the 3D seismic volume away from the well.

We interpret the interval riddled with calcite veins as a thrust zone, wider than 100 m, containing the two massive sandstones encased in deformed claystones. These sandstones cannot derive from the immediate wall-rock encountered with high claystone content in the well. There are two other general origins: as fault-bounded slices displaced in the main thrust zone (e.g., Butler and McCaffrey, 2004) or as injectites emplaced along the thrust zone (e.g., Palladino et al., 2016). We favor the first option. Borehole image log data show that shear planes or folded bedding planes dipping sub-parallel to the thrust zone are present within the sandstones (Fig. 3). This supports faulting as the emplacement mechanism and would not be associated with injectites that often display little deformations. The X-reflector occurs only between the footwall and hanging wall cut-offs of the Fan A; the injectites would be expected to extend beyond these cut-offs.

The geological interpretation of the X-reflector as entrained sandstone slices may now be extrapolated from the well into the 3D seismic volume. In the northern sector, these slices are segmented into non-collinear reflections (Fig. 2), suggesting that the sandstones are distributed along vertically stacked or relaying subsidiary fault segments within the thrust zone. The X-reflector is more continuous to the south, suggesting that subsidiary fault segments are connected (Fig. 2). The southernmost section is marked by a narrow distribution of the X- reflection, probably due to diminished displacement on the thrust zone and a change in the property of the host rock.

PRESSURE COMMUNICATION ACROSS THE THRUST ZONE

The impact of the sand slices on the hydrodynamic behavior of the thrust zone can be investigated through pore-pressure profiles for the adjacent claystones. These were calculated using resistivity, sonic and density logs by applying both Eaton and Depth Equivalent methods. A regional normal compaction trend for the claystones was generated from other wells elsewhere that penetrate the seismic volume. The pore-pressure predictions suggest that the lower 2-km section of the borehole is an over-pressured zone and the magnitude of over-pressure increases stepwise with depth (Fig. 4). The thrust zone is located at an interval where the pore-pressure gradient drops sharply from c. 12 psi/m to 2 psi/m. This indicates that the thrust zone acts as a pressure baffle or even barrier keeping the footwall highly over-pressured today despite the sandstone occurrences over the fault surface. Porous sandstones are unlikely to achieve such behaviors – indeed, outside the thrust zone, the adjacent claystones show consistent changes in pressure with depth. It is the calcite cements that presumably account for the current hydro-dynamic behavior of the thrust zone.

THE ORIGIN OF SAND SLICES AND IMPLICATIONS FOR THE THRUST ZONE FORMATION

Given that the X-reflector represents concentrations of sand slices within the thrust zone, we infer that they mainly originate from the thick sandstone sequence of Fan A in the Upper Miocene, pre-kinematic succession (Fig. 5). They result from the thrust zone not forming a single discrete plane, but by connection of discrete fault segments to form an anastomosing network of subsidiary thrusts.

Similar patterns of fault-bounded sand slices have been described from outcrops in SE France (Butler and McCaffrey, 2004). Here thrusts have formed in Oligocene turbidites that accumulated adjacent to the ancestral Alpine mountain belt and are exposed on km-high hillsides. The thrust zones climb across multilayers defined by variations in the proportions of sandstone beds relative to siltstones with a displacement of c. 1 km. The sandstones form 80 m thick of packages at most. The thrust ramps contain displaced slices that in many cases can be correlated directly with their intact counterparts on either side of the thrusts. Their bounding fault surfaces connect with the main thrust zones.

Butler and McCaffrey (2004) propose that the architectural complexities of the thrust zones in the Alps are a consequence of the deformation localization through the sandstone/siltstone multilayers. The main thrust zone grew through the growth and connection of small faults that originated as spatially isolated strands developed preferentially in the thick sandstone units. With increasing strain, these segments then anastomosed in a manner previously envisaged by Eisenstadt and De Paor (1987). These complex localization behaviors appear to be especially common for thrusts in sedimentary multilayers.

In the NW Borneo, up to 80 m thick of sandy turbidite packages are offset, as seen in the SE France example. However, the thrust zone in the NW Borneo reaches displacement of c. 2 km, almost double of that predicted in the SF France outcrop. Considering the higher displacement-to-sandstone thickness ratio in the Borneo area (~25), the sandstone slices would be dispersed between the hanging wall and footwall cut-offs of the Fan A in forms of more smeared, torn-off lenses than in SE France (Fig. 5). The X-reflector may originate from such a set of sandstone lenses rather than a single sandstone layer located all along the thrust fault.

CONCLUSIONS

By linking high-resolution 3D seismic imaging to petrophysical and lithological data derived from a well penetration, we have shown that an extensive fault-plane reflection from a deep-water thrust zone originates from entrained sandstones. Unlike many other such reflections, it has a positive polarity in contrast to negative signatures of those from fault planes thought to originate from anomalous overpressure. The thrust zone nevertheless acts as a pressure baffle. The reflectivity is enhanced by the juxtaposition against claystones and the presence of porosity-occluding calcite cements in the sandstone slices. The calcite cement provides a mechanism for containing elevated pore-pressures below the thrust zone. However, the occurrences of calcite veins indicate an earlier period of enhanced fluid fluxing in the thrust zone. The increased resistivity and sonic logs support such abundant cementation associated with the active fluid flow within the thrust zone. The complexity of fault zone architecture and presumably the inferred complexity of hydrodynamic behavior may be typical of thrusts developed in stratigraphic multilayers, such as the stacked turbidite successions of deep-water systems.

This study may inform the interpretation of fault-plane reflections obtained from thrust zones developed in turbidite successions elsewhere.

ACKNOWLEDGMENTS

This work is part of Ph.D. research supported by INPEX CORPORATION at University of Aberdeen. We thank Conrad Childs, Haakon Fossen, and an anonymous reviewer for their reviews and constructive suggestions. We thank Petronas and INPEX CORPORATION for the provision of seismic and well data to the Ph.D. research, and for permission to publish this work. Schlumberger and Midland Valley are thanked for the academic use of Petrel 2016.1 and Move 2017.2 software.

REFERENCES CITED

Butler, R.W.H., and McCaffrey, W.D., 2004, Nature of thrust zones in deep water sand-shale sequences: Outcrop examples from the Champsaur sandstones of SE France: Marine and Petroleum Geology, v. 21, p. 911–921, https://doi.org/10.1016/j.marpetgeo.2003.07.005.

Caine, J.S., Evans, J.P., and Forster, C.B., 1996, Fault zone architechture and permeability structure: Geology, v. 24, p. 1025–1028, doi:10.1130/0091-7613(1996)024<1025.

Childs, C., Manzocchi, T., Walsh, J.J., Bonson, C.G., Nicol, A., and Schöpfer, M.P.J., 2009, A geometric model of fault zone and fault rock thickness variations: Journal of Structural Geology, v. 31, p. 117–127, https://doi.org/10.1016/j.jsg.2008.08.009.

Chopra, S., and Marfurt, K.J., 2005, Seismic attributes—A historical perspective: Geophysics, v. 70, p. 3SO–28SO, doi:10.1190/1.2098670.

Eisenstadt, G., and De Paor, D.G., 1987, Alternative model of thrust-fault propagation: Geology, v. 15, p. 630–633, https://doi.org/10.1130/0091-7613(1987)15<630:AMOTP>2.0.CO;2.

Faulkner, D.R., Jackson, C.A.L., Lunn, R.J., Schlische, R.W., Shipton, Z.K., Wibberley, C.A.J., and Withjack, M.O., 2010, A review of recent developments concerning the structure, mechanics and fluid flow properties of fault zones: Journal of Structural Geology, v. 32, p. 1557–1575, https://doi.org/10.1016/j.jsg.2010.06.009.

Hutchison, C.S., 2005, Geology of North-West Borneo: Sarawak, Brunei and Sabah: Elsevier.

Iacopini, D., Butler, R.W.H., Purves, S., McArdle, N., and De Freslon, N., 2016, Exploring the seismic expression of fault zones in 3D seismic volumes: Journal of Structural Geology, v. 89, p. 54–73, https://doi.org/10.1016/j.jsg.2016.05.005.

Kolyukhin, D.R., Lisitsa, V.V., Protasov, M.I., Qu, D., Reshetova, G.V., Tveranger, J., Tcheverda, V.A., and Vishnevsky, D.M., 2017, Seismic imaging and statistical analysis of fault facies models: Interpretation (Tulsa), v. 5, p. SP71–SP82, https://doi.org/10.1190/INT-2016-0202.1.

Moore, J.C., Moore, G.F., Cochrane, G.R., and Tobin, H.J., 1995, Negative-polarity seismic reflections along faults of the Oregon accretionary prism: Indicators of overpressuring: Journal of Geophysical Research. Solid Earth, v. 100, p. 12895–12906, https://doi.org/10.1029/94JB02049.

Palladino, G., Grippa, A., Bureau, D., Alsop, G.I., and Hurst, A., 2016, Emplacement of sandstone intrusions during contractional tectonics: Journal of Structural Geology, v. 89, p. 230–249, https://doi.org/10.1016/j.jsg.2016.06.010.

Park, J.-O., Tsuru, T., Kodaira, S., Cummins, P.R., and Kaneda, Y., 2002, Splay Fault Branching Along the Nankai Subduction Zone: Science, v. 297, p. 1157–1160, https://doi.org/10.1126/science.1074111.

Schlumberger, 1991, Log Interpretation Principles/Applications: Houston, Schlumberger Educational Services, https://www.slb.com/resources/publications/books/lipa.aspx

Shipton, Z.K., and Cowie, P.A., 2003, A conceptual model for the origin of fault damage zone structures in high-porosity sandstone: Journal of Structural Geology, v. 25, p. 333–344, https://doi.org/10.1016/S0191-8141(02)00037-8.

Shipton, Z.K., and Cowie, P.A., 2001, Damage zone and slip-surface evolution over μm to km scales in high-porosity Navajo sandstone, Utah: Journal of Structural Geology, v. 23, p. 1825–1844, https://doi.org/10.1016/S0191-8141(01)00035-9.

Torabi, A., Alaei, B., Kolyukhin, D., Libak, A., Gabrielsen, R.H., and Braathen, A., 2016, Fault geometric and seismic attributes: An integrated study with focus on the Barents Sea: First Break, v. 34, p. 51–58.

Torabi, A., and Berg, S.S., 2011, Scaling of fault attributes: A review: Marine and Petroleum Geology, v. 28, p. 1444–1460, https://doi.org/10.1016/j.marpetgeo.2011.04.003.

Totake, Y., Butler, R.W.H., Bond, C.E., and Aziz, A., 2018, Analyzing structural variations along strike in a deep-water thrust belt: Journal of Structural Geology, v. 108, p. 213–229, https://doi.org/10.1016/j.jsg.2017.06.007.

FIGURE CAPTIONS

Figure 1. Study data set in the offshore NW Borneo. (a) A perspective view of the 3D seismic survey with time elevation map of top pre-kinematic strata (horizon h4) and well data. Red-filled rectangle in the inset shows the location of seismic survey. (b) A structural interpretation of a representative seismic cross-section. White arrows show a locally distributed positive-impedance contrast (the X-reflector) along the thrust zone.

Figure 2. Spatial distribution of the X-reflector on the thrust zone. The X-reflector largely occurs between fault cut-offs of reflective stratal packages termed Fan A. The X-reflector changes its extent and its continuity along strike, becomes segmented in the northern section as white arrows highlight.

Figure 3. Well-seismic correlation of Well Z. The thrust zone comprises steeply dipping claystones and massive sandstones. The X-reflector derives from the top of the sandstones showing high resistivity and fast acoustic sonic logs in the thrust zone. Sst = Sandstone and Clst = Claystone.

Figure 4. Pore-pressure prediction for Well Z. An abrupt change in pore-pressure implies the thrust zone behaves as a baffle or a barrier keeping the footwall overpressured.

Figure 5. An interpretation of the thrust zone of the Borneo data set. Sandstone slices are entrained along an anastomosing thrust network that accommodates displacement of c. 2 km. Such structural complexity and lithological heterogeneity are likely to be common in

sedimentary multilayers due to strain localization controlled by mechanical stratigraphy.

Display at no vertical exaggeration.

Figure 1

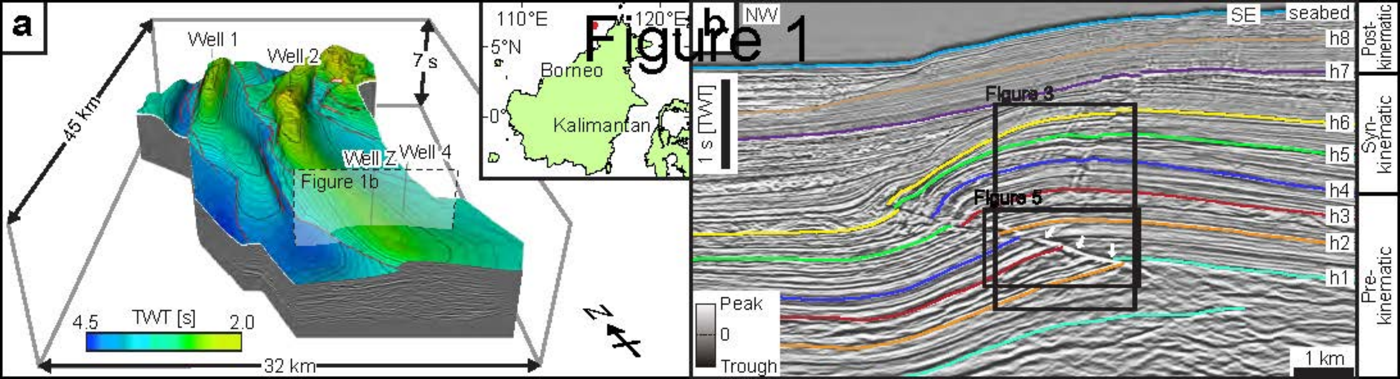

a
Well 1
Well 2
7 s
45 km
Well Z
Well 4
Figure 1b
TWT [s]
4.5
2.0
32 km
N
110°E
120°E
5°N
0°
Borneo
Kalimantan
b
NW
SE
seabed
h8
h7
h6
h5
h4
h3
h2
h1
Post-kinematic
Syn-kinematic
Pre-kinematic
1 s [TWT]
Figure 3
Figure 5
Peak
0
Trough
1 km

Figure 2

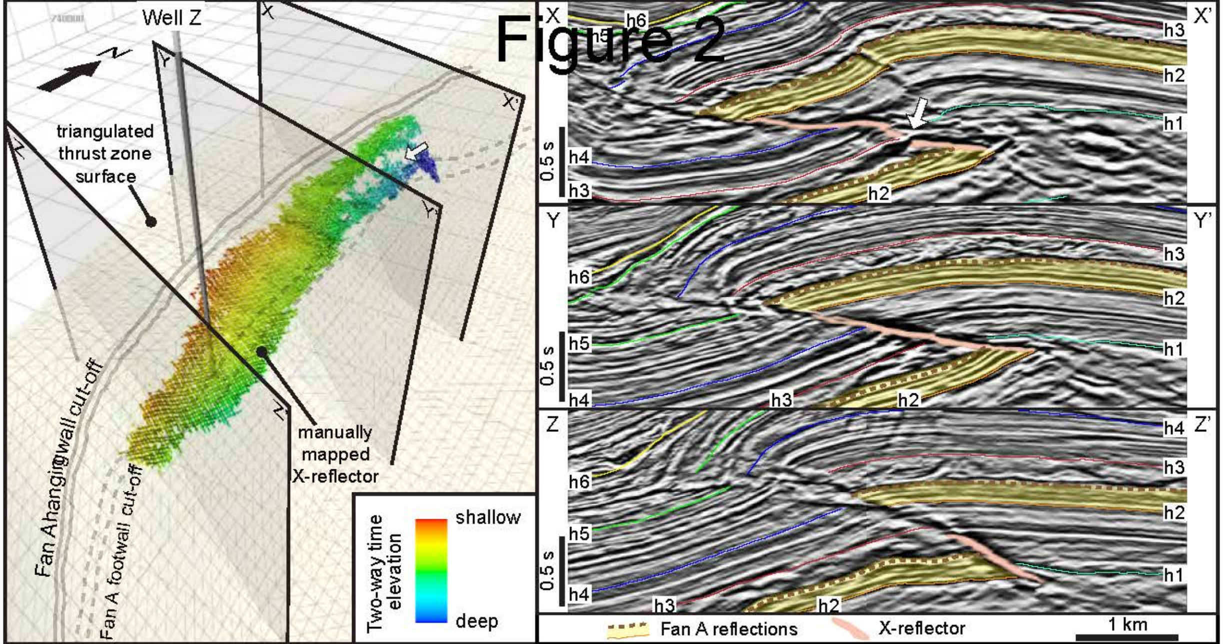

Well Z
X
Y
X'
Y'
Z
Z'
triangulated
thrust zone
surface
manually
mapped
X-reflector
Fan A hanging wall cut-off
Fan A footwall cut-off
Two-way time
elevation
shallow
deep
X
X'
h6
h5
h3
h2
h1
h4
h3
h2
0.5 s
Y
Y'
h6
h3
h2
h5
h1
h4
h3
h2
0.5 s
Z
Z'
h4
h3
h6
h2
h5
h1
h4
h3
h2
0.5 s
Fan A reflections
X-reflector
1 km

Figure 3

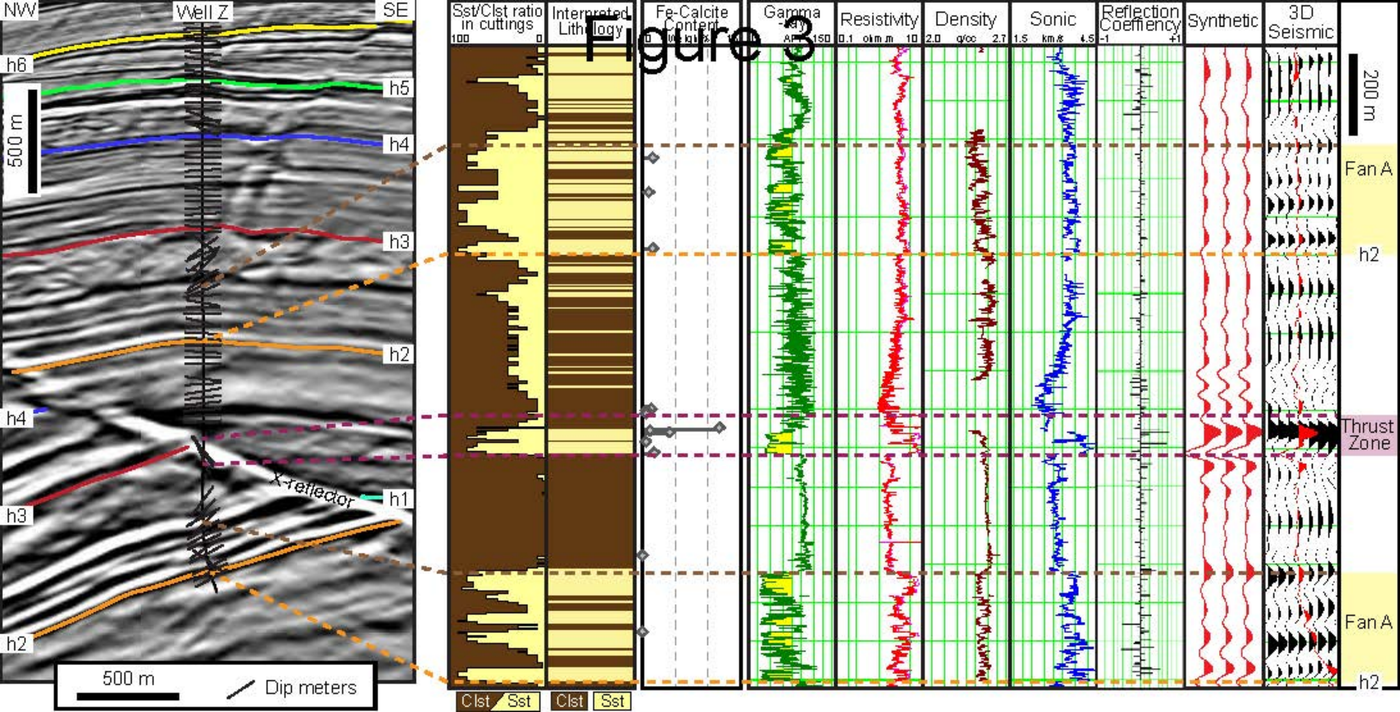

NW
Well Z
SE
h6
h5
500 m
h4
h3
h2
h4
h1
X-reflector
h3
h2
500 m
Dip meters
Sst/Clst ratio in cuttings
100
0
Interpreted Lithology
Fe-Calcite Content
Gamma -ray
API
150
Resistivity
0.1
ohm.m
10
Density
2.0
g/cc
2.7
Sonic
1.5
km/s
4.5
Reflection Coefficiency
-1
+1
Synthetic
3D Seismic
200 m
Fan A
h2
Thrust Zone
Fan A
h2
Clst
Sst
Clst
Sst

Figure 4

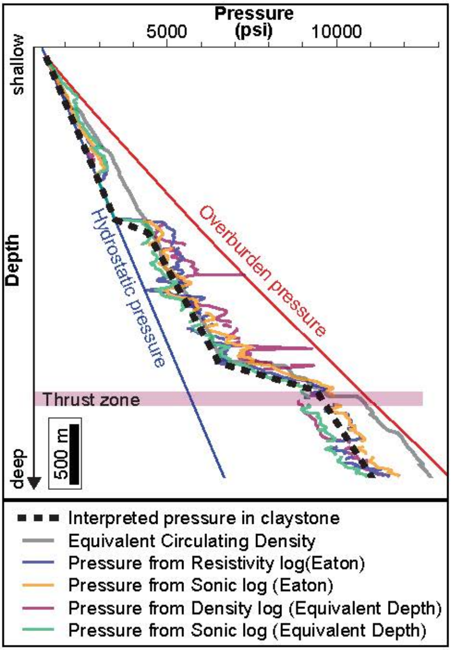

Pressure
(psi)
5000
10000
shallow
Depth
deep
Overburden pressure
Hydrostatic pressure
Thrust zone
500 m
Interpreted pressure in claystone
Equivalent Circulating Density
Pressure from Resistivity log(Eaton)
Pressure from Sonic log (Eaton)
Pressure from Density log (Equivalent Depth)
Pressure from Sonic log (Equivalent Depth)

Figure 5

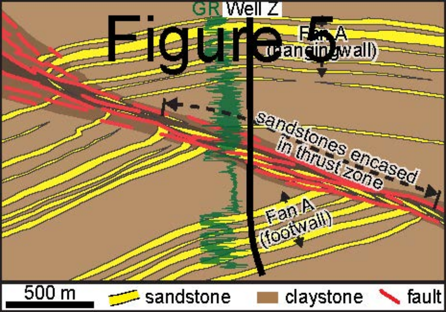
GR
Well Z
Fan A
(hangingwall)
sandstones encased
in thrust zone
Fan A
(footwall)
500 m
sandstone
claystone
fault